J Mater Sci (2006) 41:7240–7246
DOI 10.1007/s10853-006-0914-x

# High temperature, spectral-directional emittance of high purity nickel oxidized in air

**George Teodorescu · Peter D. Jones · Ruel A. Overfelt · Baojian Guo**

Received: 22 September 2005 / Accepted: 12 December 2005 / Published online: 7 October 2006


**Abstract** Spectral-directional emittance measurements for 99.99% nickel, thermally oxidized in air, were performed at temperatures of 673, 773, and 873 K using an apparatus comprised of a Fourier transform infrared (FTIR) spectrometer, a blackbody radiating cavity (hohlraum), and a sample holder which allows directional measurements. The data cover the spectral range between 2 and 20 μm, and the directional range from a surface normal to 72° polar angle. The Ni sample had a nominal surface roughness of 4.1 μm and was heated for 1 h at the measurement temperatures prior to emission measurements. X-ray diffraction and EDS analyses were performed in order to characterize the sample surface. It was found that the normal emittance of oxidized nickel increases with temperature for the temperature range considered. Directional emittance shows slightly departure from pure metal behavior.

**Nomenclature**

| | |
|---|---|
| $\epsilon_\lambda$ | spectral emittance |
| $I_\lambda$ | spectral intensity, W/ ($m^2$ μm sr) |
| $\lambda$ | wavelength, μm |
| $T$ | temperature, K |
| $k$ | direction vector |
| $\theta$ | polar angle |
| $\delta\epsilon$ | emittance uncertainty |
| $\delta$T | temperature uncertainty, K |
| $c_2$ | second radiation constant, μm K |
| $h$ | Planck's constant, J s |
| $c_0$ | speed of light in vacuum, m/s |
| $K$ | Boltzmann's constant, J/K |

**Subscripts**

| | |
|---|---|
| b | blackbody |
| s | sample surface |
| r | surroundings visible to sample surface |

G. Teodorescu (✉) · R. A. Overfelt · B. Guo
Department of Mechanical/Materials Engineering, Auburn University, 275 Wilmore, Auburn, AL 36849-5341, USA
e-mail: teodoge@auburn.edu

R. A. Overfelt
e-mail: overfra@auburn.edu

B. Guo
e-mail: guobaoj@auburn.edu

P. D. Jones
Department of Mechanical Engineering, Auburn University, 201 Ross Hall, Auburn, AL 36849-5341, USA
e-mail: pjones@eng.auburn.edu

## Introduction

Thermal properties of high purity nickel are of great importance and interest in radiative heat transfer applications in the aerospace industry for critical parts such as turbine blades and discs in jet engines, as well as in other devices and industries. Accurate prediction of the behavior of high purity nickel at high temperatures in air depends on knowledge of its radiative properties, which themselves depend upon surface roughness, composition, aging, temperature, wavelength, and direction. Emittance is an important radiative property that facilitates pyrometric measurements and numerous

thermal computations. The emittance of the opaque surface of a material is defined as:

$$\varepsilon_{\lambda}(T,\lambda,\hat{k}) \equiv \frac{I_{\lambda}(T,\lambda,\hat{k})}{I_{\lambda b}(T,\lambda)} \quad (1)$$

where $I_{\lambda}(T,\lambda,\hat{k})$ is the spectral emitted intensity which leaves the surface at a specific wavelength $\lambda$ and temperature $T$, into a direction $\hat{k}$, and $I_{\lambda b}(T,\lambda)$ is the spectral emitted intensity which leaves a blackbody at the same wavelength and temperature.

The total emissivity of oxidized nickel was reported by Randolph and Overholzer [1] for a polished nickel surface oxidized at temperatures of 473, 673 and 873 K. They used metal disc samples of 19.1 cm diameter and 6 to 13 mm thickness. Thermocouples attached to the back of the metal sample were used to measure sample temperature, not the surface temperature itself. The nickel samples used in their experiment were oxidized at 873 K until the emissivity had become constant prior to taking measurements at the above mentioned temperatures. Using a potentiometer a calibration was performed, showing the relation between millivolts and energy radiated by a blackbody cavity. The blackbody—a cast iron pipe, had a uniform wall temperature within 3 K at 500 °C. Data from [1] give no information about spectral or directional emittance of oxidized nickel and topology of metal's surface. Furthermore, the surface composition was not quantified. Clausen et al. [2] report normal spectral emissivity of an oxidized nickel specimen below 390 K for a spectral range 2.8–5.7 μm. They used a specimen of lightly oxidized nickel with dimensions 20 × 20 × 1 mm provided by NPL England. The specimen had a normal emissivity at 773 K of 0.64 at 3.18 μm and 0.57 at 5.06 μm given by the provider. The authors do not specify the sample preparation, initial composition and surface roughness. The emittance reported in ref. [2] is limited to normal and the spectral range is too narrow. Bauer et al. [3] determined the normal spectral emissivity of sand blasted pure nickel in vacuum for a spectral range of 0.6 to 16 μm at 673 K using a radiometric technique with a separate blackbody. The measurement device was comprised of a prism monochromator, three different detectors and a Lock-in-Amplifier. Although there is some data in literature [1, 2] on total emittance and spectral normal emittance of oxidized nickel a correlation cannot be performed because the sample surface preparation is not well quantified, the spectral range is very limited and no spectral-directional emittance of oxidized nickel was reported.

The objective of this study is to determine the spectral-directional emittance of high purity nickel (99.99%) in air with known surface roughness after various heat treatments using an FTIR spectrometer, which is a powerful instrument for measuring the emittance spectra at high spectral resolution. The measurement temperature range considered here is between 673–873 K and the spectral range from 2 to 20 μm. Directional data range from a surface normal to 72° polar angle. Such emittance data are required for use in radiation heat transfer, which account for emittance variation with direction, wavelength and temperature. The measurements were carried out by comparing the radiation heat fluxes of the sample and the blackbody cavity both maintained at the same temperature.

## Experimental apparatus

The nickel sample provided by ALFA AESAR was mounted on a temperature controlled heater block. The heater block and the sample are heavily insulated up to the plane of sample surface. The heater block, the sample and the insulation are contained in a slotted arc rack casing (Fig. 1, item 1). The sample surface temperature was monitored and controlled by a thermocouple that was embedded through the heater into the sample up to a point just beneath the sample-radiating surface. A Perkin Elmer FTIR spectrometer (Spectrum GX) was used to replace the optical discrimination and detection systems of a previous apparatus, capable of making spectral-directional emittance measurements, which is described in refs. [4–6]. Radiative flux is measured within a finite solid angle of 0.0049 steradian (str) using a 12 mm aperture. The radiation, which leaves the sample (2), is reflected from an off-axis parabolic gold-coated mirror (4) into a collimated beam (6). The collimated beam is then directed into an FTIR spectrometer (7) using the external FTIR spectrometer viewport. The optical path is calibrated using a blackbody cavity, which is positioned at 90° from the sample and can be viewed by rotating the gold-coated parabolic mirror. The blackbody-radiating cavity was machined into 152 mm diameter copper round stock, insulated by a 76 mm thick ceramic wool blanket and its wall temperature was kept at the same temperature as the sample surface using a PID temperature controller. By rotating the parabolic off-axis mirror (4) using a rotation mechanism (5) and moving the sample position to a corresponding position on the slotted

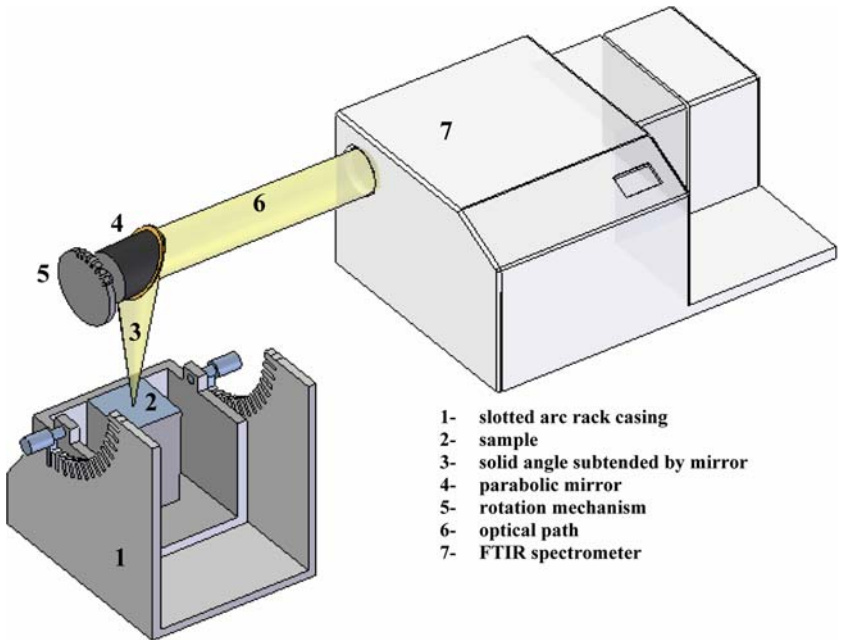


**Fig. 1** Schematic of experimental setup

arc rack, measurements at different angles to the surface normal were achieved.

The experimental setup was tested for accuracy with pure alumina (99.5% provided by Morgan Advanced Ceramics) at 823 K. The data obtained (Fig. 2) showed good agreement with data published by Vader et al. [7]. The data represent an average of three measurements of ten scans with a resolution of 16 $cm^{-1}$, each collected at different times.

Subsequently XRD analysis performed on the sample indicated the presence of nickel oxide on the surface as shown on X-ray diffraction pattern in Fig. 3.

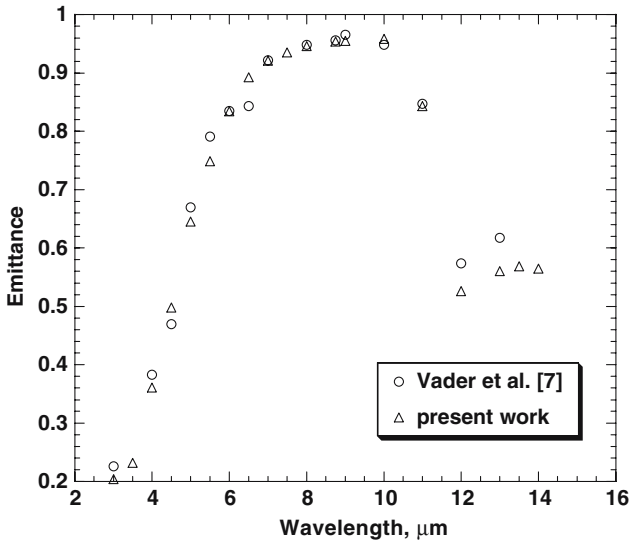


**Fig. 2** Comparison of spectral-normal emittance of alumina (99.5%) with Vader's et al. [7]

The first three strongest reflections were identified for nickel oxide, which has a cubic structure. The corresponding peaks identified for (111), (200) and (220) planes are seen in Fig. 3. Furthermore, the EDS analysis performed on the sample surface indicated an O/Ni atomic concentration ratio of approximately $r = 1$ which is associated with NiO phase. The micrograph of the oxidized nickel sample in Fig. 4b, d show significant modifications as a result of nickel oxide grains formed on the sample surface (Fig. 4a, c).

## Measurement procedure

Samples of pure nickel plate (99.99%), 75 × 75 × 6 mm thick, polished smooth, with a nominal surface roughness of 4.1 μm., were used in the experiment. A heat transfer analysis showed a difference of no more than 1 K between the measurement point and the actual surface temperature. The actual surface temperature is the temperature of the exposed to air surface which was calculated according to [5], which considers a temperature gradient in the oxidized nickel sample, convection, and radiation. The sample surface was brought from room temperature to 673 K and maintained at 673 K for 1 h prior to taking emission measurements to allow oxidation. Afterwards, the sample surface temperature was increased by a step increment of 100 K until a maximum temperature of 873 K was attained. The radiation heat flux, which leaves the sample from an area of the plane surface, was collected by the parabolic gold-coated collector, which has a focal length of 76.2 mm. The radiation is then collimated

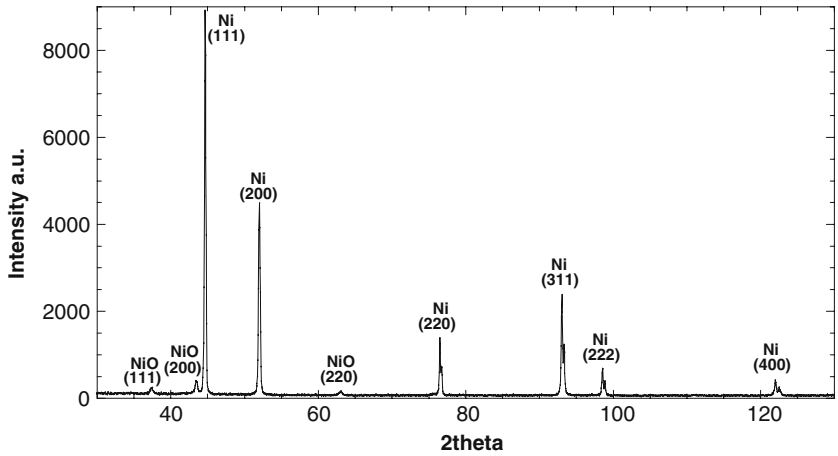


**Fig. 3** X-ray diffraction pattern of oxidized nickel

by the parabolic collector into the optical path toward the FTIR spectrometer external viewport. The spectral-directional emittance $\epsilon$ is determined according to [8]:

$$\varepsilon(\lambda, \theta, T_s) = \frac{I_s(T_s, \lambda, \theta) - I_b(T_r, \lambda)}{I_b(T_b, \lambda) - I_b(T_r, \lambda)} \quad (2)$$

where, $I_s(T_s,\lambda,\theta)$ is the intensity emitted by the sample surface at temperature $T_s$, $I_b(T_b,\lambda)$ is the intensity emitted by the blackbody cavity at temperature $T_b$ (which is equal to the sample surface at temperature $T_s$), and $I_b(T_r,\lambda)$ is the intensity emitted by the surrounding at room temperature, $T_r$ The emissivity is evaluated according to Eq. 2, taking into account the following assumptions:

1. The solid angle over which the emission signal is collected is very small, and the spectral intensity is assumed to be constant within this solid angle.
2. The blackbody cavity is perfectly black, which means that the blackbody is isothermal and its aspect ratio and aperture size produce an effective emissivity of unity.
3. The sample and blackbody surfaces are isothermal during the radiation signal measurement.
4. The broadband intensity emitted from the sample surface is unpolarized.

The maximum optical thickness value determined for nickel oxide layer thermally grown on nickel surface was found to be about $2.4 \times 10^{-6}$ which suggests that the nickel oxide is optically thin. The absorption

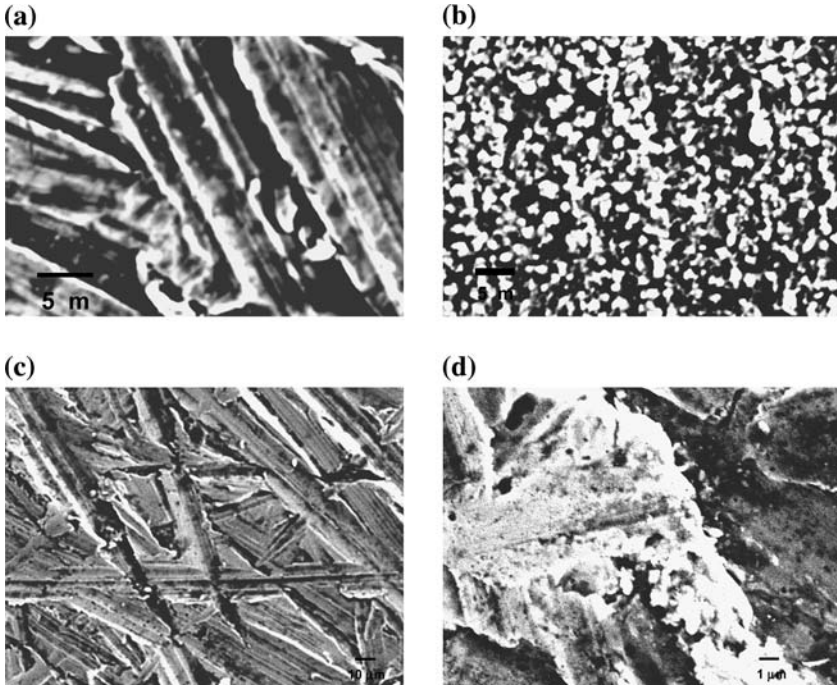


**Fig. 4** SEM microstructure of nickel sample. (**a**) as received 2000×, (**b**) oxidized sample 2000×, (**c**) as received 4000×, (**d**) oxidized sample 4000×

coefficient of nickel oxide used to determine the optical thickness was reported by Newman and Chrenko [9] at 300 K. We mention that absorption coefficient of nickel oxide at our measurement temperature data was not available. The thickness of nickel oxide layer used to compute the optical thickness was evaluated according to Atkinson [10] to be about 600 nm.

The uncertainty in the emittance value $\delta\epsilon$ is given according to [11]:

$$\delta\varepsilon_\lambda = \varepsilon_\lambda \frac{\delta T}{\lambda T_s^2} \frac{c_2}{[\exp(-c_2/\lambda T_s) - 1]} \quad (3)$$

where $\lambda$ is the wavelength, and $c_2 = hc_0/K$. According to Eq. 3, the relative uncertainty is inversely proportional to $\lambda T_s^2$, resulting in a maximum uncertainty at lower temperatures and shorter wavelengths. The temperature uncertainty is comprised of the uncertainty of the blackbody temperature, sample surface temperature and the stability of the temperature control. Uncertainties for type J special thermocouples used in experiment reported by manufacturer (Watlow Controls) were 0.4% and 0.05% for temperature control stability (Series 965 auto tuning control). The uncertainty estimation procedure from Moffat [12] was used to determine the total estimated uncertainty as shown in Table 1. The maximum uncertainty in the emittance value was found to be less than 3.5% for the spectral range considered.

## Results and discussion

Figure 5 shows spectral-normal emittance data at all three considered temperatures. The spectral-normal emittance is seen to increase very slightly with temperature from 673 to 873 K as shown in Fig. 5. A very important key feature observed here is the apparition of two slight peaks (the plot magnitude is decreased to enhance the peaks for better visualization). These peaks observed at wavelengths of 9.5 and 15 μm were attributed to nickel oxide grown on the sample surface.

Figure 6 shows emittance data as a function of direction at various wavelengths for 99.99% nickel oxidized at 873 K for 1 h. From Fig. 6 it can be distinguished that for spectral range from 17 to 20 μm, the directional emittance increases slightly with direction and the increase is more pronounced at angles higher than 30°. This behavior does not agree with pure

**Table 1** Uncertainty estimates of the emissivity measurement

| Parameter | Estimated $\pm 2\sigma$ confidence limits(%) | Emissivity change at $\lambda$ = 2 μm | Emissivity change squared $*10^6$ |
|---|---|---|---|
| Sample surface temperature | 0.4 | 0.0038 | 14.4 |
| Blackbody temperature | 0.4 | 0.0038 | 14.4 |
| Stability of the BB temperature | 0.05 | 0.0004 | 0.16 |
| Stability of sample temperature | 0.05 | 0.0004 | 0.16 |
| Total uncertainty in emissivity $[\Sigma(\delta\mu i)^2]^{1/2}$ | | | 0.0051 |
| Total % uncertainty in emissivity ($\epsilon$ = 0.151, at $T$ = 400 °C) | | | 3.4% |

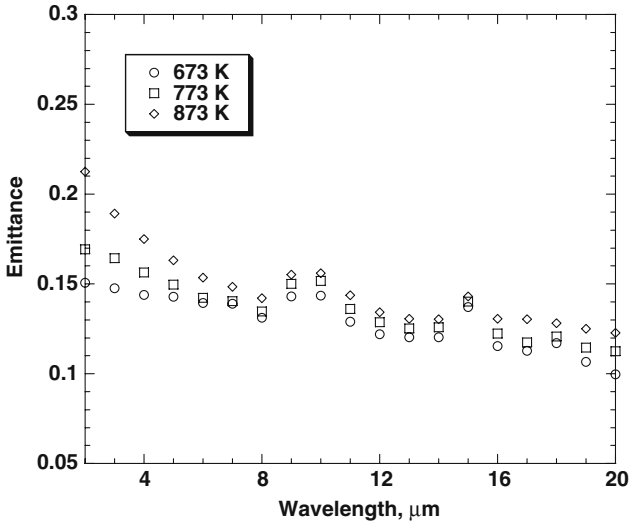


**Fig. 5** Measured normal spectral-directional emittance of oxidized 99.99% Ni at 673,773 and 873 K

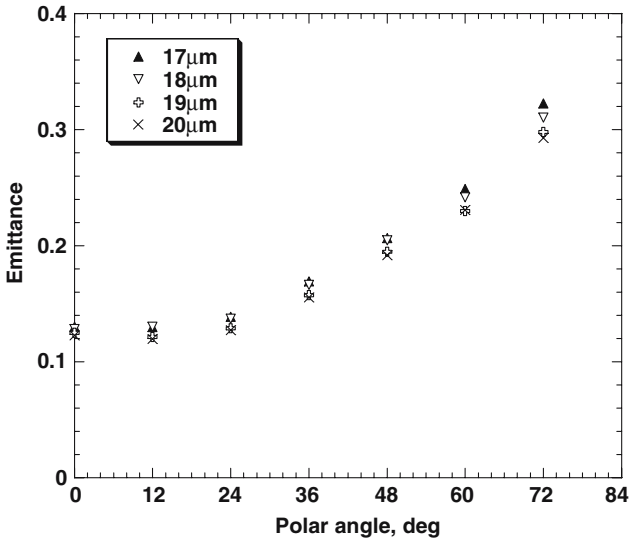


**Fig. 6** Measured spectral-directional emittance of oxidized 99.99% Ni at 873 K

metals behavior, which states that directional emittance is almost constant for polar angles less than 40°, suggesting that radiative properties of pure nickel are slightly altered by the nickel oxide grown on the surface.

Figure 7 shows the normal-spectral emittance of nickel oxidized in air at 673 K for 1 h, with a surface roughness of 4.1 μm, from present work and the spectral-normal emissivity of pure nickel reported by Bauer et al. [3], at the same temperature. The Bauer et al. [3] measurement was performed in a vacuum controlled atmosphere to avoid oxidation at high temperatures. Comparing these two sets of data it can be observed that the magnitude of the spectral-normal emittance of nickel oxidized in air is higher than that presented in [3] for nickel heated in vacuum in controlled gas atmosphere. Clearly this can be influenced by the nickel oxide grown in air on the surface, and the surface roughness. Unfortunately, Bauer et al. [3] did not report the surface roughness in order to make an inference.

Furthermore, the two slight peaks observed in the spectral-normal emittance from present work were not observed in [3] because of the vacuum controlled environment, which help us attribute them to nickel oxide grown on the surface over a 1 h period of heating. The spectral-directional emittance data are presented in Table 2.

The spectral hemispherical emittance was determined by integrating the present data over polar angle.

Figure 8 shows spectra for different temperatures suggesting that the spectral hemispherical emittance of

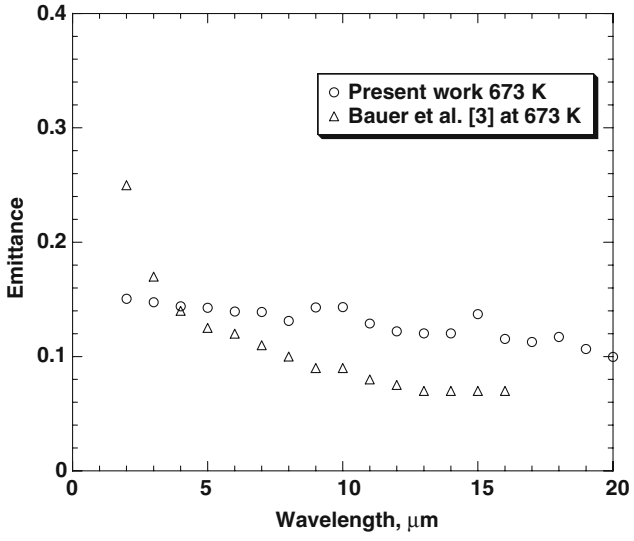


**Fig. 7** Spectral-normal emittance comparison

**Table 2** Measured spectral-directional emittance of oxidized nickel at 673 K (1st row), 773 K (2nd row) and 873 K (3rd row)

| λ, μm | Polar angle, degree | | | | | | |
|---|---|---|---|---|---|---|---|
| | 0° | 12° | 24° | 36° | 48° | 60° | 72° |
| 2 | 0.151 | 0.174 | 0.169 | 0.172 | 0.200 | 0.202 | 0.242 |
| | 0.169 | 0.184 | 0.190 | 0.203 | 0.201 | 0.216 | 0.184 |
| | 0.213 | 0.228 | 0.235 | 0.248 | 0.254 | 0.258 | 0.242 |
| 3 | 0.147 | 0.168 | 0.177 | 0.185 | 0.193 | 0.210 | 0.220 |
| | 0.164 | 0.179 | 0.184 | 0.193 | 0.202 | 0.213 | 0.219 |
| | 0.189 | 0.209 | 0.218 | 0.231 | 0.242 | 0.251 | 0.253 |
| 4 | 0.143 | 0.164 | 0.176 | 0.181 | 0.191 | 0.199 | 0.212 |
| | 0.156 | 0.171 | 0.176 | 0.184 | 0.195 | 0.208 | 0.218 |
| | 0.175 | 0.192 | 0.200 | 0.214 | 0.226 | 0.237 | 0.246 |
| 5 | 0.143 | 0.158 | 0.170 | 0.178 | 0.185 | 0.195 | 0.210 |
| | 0.150 | 0.162 | 0.168 | 0.175 | 0.186 | 0.199 | 0.212 |
| | 0.163 | 0.178 | 0.185 | 0.200 | 0.211 | 0.223 | 0.237 |
| 6 | 0.139 | 0.154 | 0.165 | 0.173 | 0.181 | 0.191 | 0.211 |
| | 0.142 | 0.155 | 0.159 | 0.167 | 0.178 | 0.192 | 0.211 |
| | 0.154 | 0.167 | 0.173 | 0.187 | 0.199 | 0.212 | 0.231 |
| 7 | 0.139 | 0.152 | 0.165 | 0.170 | 0.179 | 0.188 | 0.214 |
| | 0.140 | 0.150 | 0.155 | 0.162 | 0.172 | 0.188 | 0.210 |
| | 0.148 | 0.158 | 0.164 | 0.179 | 0.191 | 0.205 | 0.228 |
| 8 | 0.131 | 0.143 | 0.155 | 0.162 | 0.170 | 0.184 | 0.209 |
| | 0.135 | 0.143 | 0.146 | 0.154 | 0.165 | 0.183 | 0.212 |
| | 0.142 | 0.151 | 0.157 | 0.175 | 0.187 | 0.202 | 0.230 |
| 9 | 0.143 | 0.156 | 0.171 | 0.186 | 0.203 | 0.227 | 0.260 |
| | 0.150 | 0.160 | 0.166 | 0.177 | 0.194 | 0.218 | 0.261 |
| | 0.155 | 0.166 | 0.174 | 0.196 | 0.219 | 0.242 | 0.278 |
| 10 | 0.143 | 0.153 | 0.170 | 0.185 | 0.202 | 0.222 | 0.255 |
| | 0.152 | 0.159 | 0.166 | 0.176 | 0.191 | 0.215 | 0.257 |
| | 0.156 | 0.166 | 0.174 | 0.195 | 0.220 | 0.243 | 0.280 |
| 11 | 0.129 | 0.136 | 0.150 | 0.161 | 0.175 | 0.195 | 0.233 |
| | 0.136 | 0.142 | 0.145 | 0.154 | 0.170 | 0.195 | 0.240 |
| | 0.144 | 0.150 | 0.157 | 0.178 | 0.201 | 0.225 | 0.268 |
| 12 | 0.122 | 0.129 | 0.140 | 0.150 | 0.163 | 0.181 | 0.218 |
| | 0.129 | 0.132 | 0.132 | 0.143 | 0.156 | 0.178 | 0.225 |
| | 0.134 | 0.139 | 0.143 | 0.164 | 0.183 | 0.204 | 0.245 |
| 13 | 0.120 | 0.127 | 0.137 | 0.148 | 0.161 | 0.180 | 0.215 |
| | 0.125 | 0.130 | 0.129 | 0.139 | 0.153 | 0.174 | 0.221 |
| | 0.131 | 0.134 | 0.138 | 0.160 | 0.179 | 0.200 | 0.242 |
| 14 | 0.120 | 0.127 | 0.137 | 0.148 | 0.161 | 0.180 | 0.215 |
| | 0.126 | 0.126 | 0.128 | 0.139 | 0.154 | 0.178 | 0.227 |
| | 0.130 | 0.132 | 0.137 | 0.158 | 0.180 | 0.204 | 0.251 |
| 15 | 0.137 | 0.141 | 0.149 | 0.170 | 0.181 | 0.194 | 0.237 |
| | 0.140 | 0.140 | 0.140 | 0.156 | 0.169 | 0.198 | 0.248 |
| | 0.143 | 0.142 | 0.148 | 0.172 | 0.198 | 0.225 | 0.277 |
| 16 | 0.115 | 0.121 | 0.131 | 0.148 | 0.162 | 0.188 | 0.232 |
| | 0.123 | 0.123 | 0.124 | 0.138 | 0.160 | 0.192 | 0.247 |
| | 0.131 | 0.131 | 0.140 | 0.167 | 0.197 | 0.232 | 0.295 |
| 17 | 0.113 | 0.117 | 0.127 | 0.143 | 0.160 | 0.184 | 0.234 |
| | 0.117 | 0.122 | 0.124 | 0.138 | 0.164 | 0.200 | 0.262 |
| | 0.130 | 0.130 | 0.139 | 0.169 | 0.206 | 0.249 | 0.323 |
| 18 | 0.117 | 0.113 | 0.126 | 0.140 | 0.158 | 0.187 | 0.235 |
| | 0.121 | 0.120 | 0.123 | 0.136 | 0.158 | 0.197 | 0.258 |
| | 0.128 | 0.130 | 0.137 | 0.166 | 0.205 | 0.242 | 0.310 |
| 19 | 0.106 | 0.111 | 0.112 | 0.136 | 0.149 | 0.172 | 0.227 |
| | 0.114 | 0.113 | 0.118 | 0.129 | 0.149 | 0.189 | 0.250 |
| | 0.125 | 0.121 | 0.129 | 0.158 | 0.195 | 0.230 | 0.298 |
| 20 | 0.100 | 0.106 | 0.110 | 0.137 | 0.146 | 0.174 | 0.227 |
| | 0.113 | 0.111 | 0.113 | 0.123 | 0.145 | 0.188 | 0.245 |
| | 0.123 | 0.120 | 0.127 | 0.155 | 0.192 | 0.231 | 0.293 |

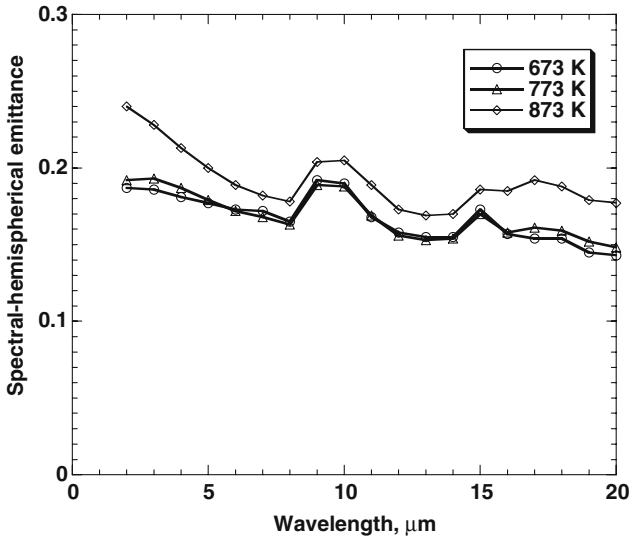


**Fig. 8** Spectral-hemispherical emittance of oxidized nickel as a function of wavelength at 673, 773 and 873 K

nickel oxidized for 1 h at 673 K and 1 h at 773 K does not change significantly. A greater temperature dependence of spectral hemispherical emittance is obvious for oxidized nickel for 1 h at 873 K. Another important features noticed on Fig. 8 are the peaks around 9.5 and 15 μm which are more significant here than on spectral-normal emittance.

## Conclusion

The spectral-directional emittance of high purity (99.99%) nickel, thermally oxidized in air at temperatures between 673 to 873 K, is determined from measurements of radiative intensity leaving the specimen. The X-ray analysis performed upon cooling the sample showed the presence of nickel oxide on the sample surface, for which the strongest three reflection peaks were identified. The spectral-normal emittance of oxidized nickel is seen to slightly increase with temperature between 673 and 873 K.

Spectral-normal emittance of oxidized nickel decreases with wavelength for spectral ranges between 2–8 μm, 11–14 μm and beyond 16 μm for all three considered temperatures. The two slight peaks observed around 9.5 and 15 μm were attributed to nickel oxide grown on the sample surface by heating in air.

**Acknowledgements** The authors gratefully acknowledge the financial support received from NASA's Space Product Development Program at Marshall Space Flight Center under Cooperative Agreement No. NCC8–240.

## References

1. Randolph CP, Overholzer MJ (1913) Phys Rev 2:144
2. Clausen S, Morgenstjerne A, Rathmann O (1996) Appl Optics 35(28):683
3. Bauer W, Oertel H, Rink M (2003) Paper presented at 15th Symposium of Thermophysical Properties. June, Boulder, Colorado
4. Jones PD, Teodorescu G, Overfelt RA, *ASME*, HT-FED2004–56050
5. Jones PD, Dorai-Raj DE, Mcleod DG (1996) J Therm Heat Trans 10(2):43
6. Teodorescu G, Jones PD, Overfelt RA and Guo Baojian, *ASME*, HT2005–72828
7. Vader DT, Viskanta R, Incropera FP (1985) Rev Sci Instr 57(1):7
8. Postlethwait MA, Sikka KK, Modest MF (1994) J Therm Heat Trans 8(3):12
9. Newman R, Chrenko RM (1959) Phys Rev 114(6):507
10. Atkinson A (1985) Rev Modern Phys 57(2):37
11. Branderberg WM, Clausen OW (1964) Int Aeros Abstr 4:313
12. Moffat RJ (1998) Exp Therm Fluid Sci 1:3